Calculations of the Soil Hot-Spot Effect Using the Coherent Backscattering Theory

Shunlin Liang and Michael I. Mishchenko†*

The shadowing theory has been widely used to account for the hot-spot effect for the canopy and soil. However, it is not valid for soils that are composed of fine particles and do not have well-defined shadows. The coherent backscattering theory is used in this study to calculate both the magnitude and the angular width of the hot-spot peak for clay and silt soils. The soil hot-spot magnitude is calculated by solving the vector radiative transfer equation. The dense nature of the soil medium is taken into account in the calculations of the hot-spot angular width. The results are also linked with the Hapke hot-spot empirical function. The effects of the wavelength dependence and of particle size and shape also are examined.

INTRODUCTION

There has been increasing interest in investigating surface bidirectional reflectance for terrestrial remote-sensing applications in recent years. One of the pronounced phenomena is the hot-spot effect—sometimes also called the opposition effect, heiligenschein, bright shadow, and so forth, in different disciplines—which is characterized by a strong reflectance peak in the solar illumination direction. The ground radiometers such as the portable apparatus for rapid acquisition of bidirectional observations of the land and atmosphere (PARABOLA) (Deering et al., 1994) and airborne sensors such as the advanced solid state array spectroradiometer (ASAS) (Irons et al., 1991; Ranson et al., 1994) and the polarization and directionality of the earth reflectances (POLDER) (Breon et al., 1996) have provided us with a lot of hot-spot data for different surface cover types. The hot-spot effect for leaf canopies has been mostly accounted for by using the shadowing theory (Kuusk, 1985; Jupp et al., 1986; Gerstl et al., 1986; Verstraete et al., 1990; Jupp and Strahler, 1991; Qin and Xiang, 1994).

Soil radiative transfer has been poorly investigated, compared with canopy radiative transfer modeling (Hapke, 1981; Lumme et al., 1990; Jacquemoud et al., 1992; Liang and Townshend, 1996a,b). The Hapke semiempirical hot-spot function simplified from the derivation based on the shadowing theory (Hapke, 1986) has been widely used for soils. According to the shadowing theory, particles that are large, compared with the wavelength, and opaque cast shadows on neighboring particles. When the viewing direction matches the illumination direction, all shadows are hidden by the particles that cast them and thus the local brightness reaches its maximum. When the viewing direction moves away from the illumination direction, shadows can be seen and the detected brightness sharply decreases.

However, the shadowing theory is not valid for soils composed of fine particles that do not have well-defined shadows. A different mechanism for the hot-spot effect from discrete random media has been suggested, which is usually known as coherent backscattering or weak photon localization. A comprehensive review of this mechanism was recently given by Barabanenkov et al. (1991). Experimental results for canopies and soils have recently been reported by Hapke et al. (1996). To explain this mechanism, let us examine Figure 1. The discrete random medium is illuminated by a scalar plane wave in the direction Ω_i. Two partial waves associated with the same incident wave travel through the same group of N scatters, denoted by $x_1, x_2, \ldots x_N$ but in opposite directions. If a is relatively large, the average effect of interference will approach zero. However, coherence is completely preserved at the backscattering direction, which results in an enhanced backscattering peak. At the backscatter-

* Laboratory of Global Remote Sensing Studies, Department of Geography, University of Maryland, College Park

† State University of New York at Stony Brook, Stony Brook and NASA / Goddard Institute for Space Studies, New York

Address correspondence to Dr. Shunlin Liang, Laboratory for Global Remote Sensing Studies, Department of Geography, University of Maryland, College Park, MD 20742.

Received 15 March 1996; revised 6 August 1996.

REMOTE SENS. ENVIRON. 60:163–173 (1997)

655 Avenue of the Americas, New York, NY 10010

0034-4257/97/$17.00
PII S0034-4257(96)00179-4

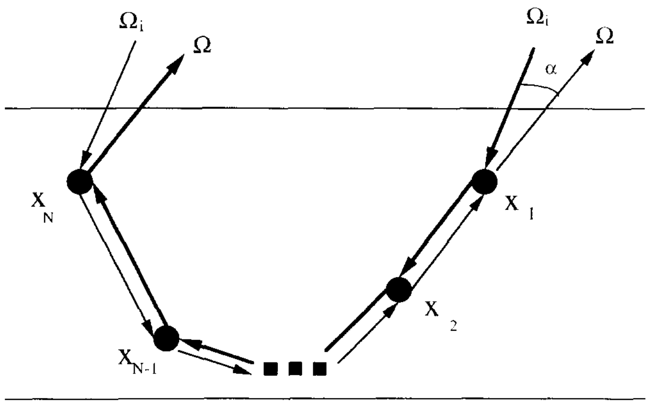

Figure 1. Schematic illustration of coherent backscattering.

ing direction (zero phase), the magnitudes of the electric fields associated with the two light paths are equal ($A_1=A_2$), and the reflected intensity is $|A_1+A_2|^2=4|A_1|^2$. In contrast, the combined intensity would be $|A_1|^2+|A_2|^2=2|A_1|^2$ in the absence of coherence. The enhancement factor is obviously 2. However, if a path involves only one particle, there is no reversed path. In other words, single scattering does not contribute to coherent enhancement. Thus, it is easy to write the enhancement factor, which is defined as the ratio of the total backscattering radiance to the incoherent (diffuse) radiance I^d:

$$\xi=\frac{I^d+I^c}{I^d}, \tag{1}$$

where the coherent radiance I^c is equal to the total incoherent radiance minus single-scattering radiance I^1 (Barabanenkov et al., 1991). Thus,

$$\xi=2-\frac{I^1}{I^d}. \tag{2}$$

Therefore, the enhancement factor is always smaller than 2. Note that this formula is valid only in the exact backscattering direction.

Although the scalar theory of enhanced backscattering outlined above is basically well understood and gives reasonably good results, it does not take into account the vector character of light and thus provides only a simplified understanding of coherent backscattering. In particular, the scalar approximation completely fails in calculating the reflected intensity in the practically important case of unpolarized incident light (Mishchenko, 1992a). Fortunately, developments of the corresponding vector theory are very encouraging. Peters (1992) proposed a vector theory of coherent backscattering for absorbing and nonabsorbing particles of a size comparable to a wavelength. A general formulation was put forward by Mishchenko (1992a), and it was found (Mishchenko and Dlugach, 1992a, 1993) in good quantitative agreement

Figure 2. Enhancement factor of the hot-spot magnitude for clay soils with different solar zenith angles at two wavelengths (0.533 μm and 0.817 μm).

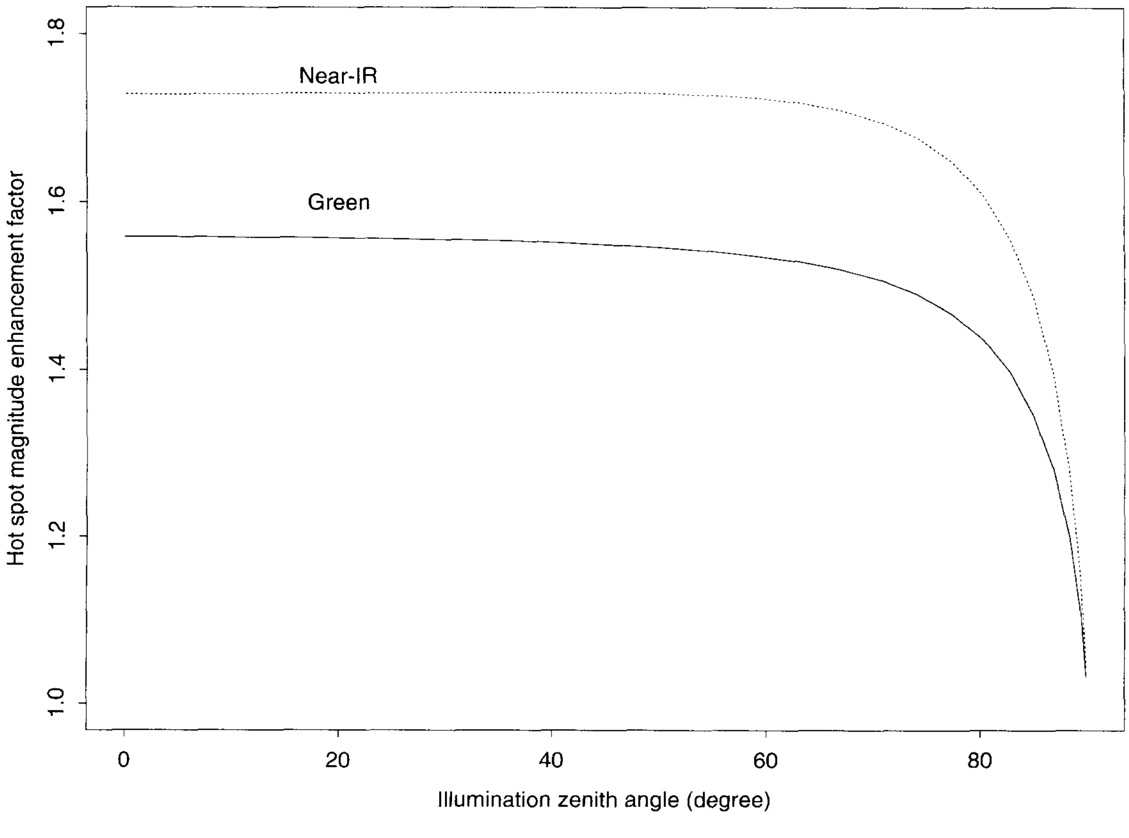

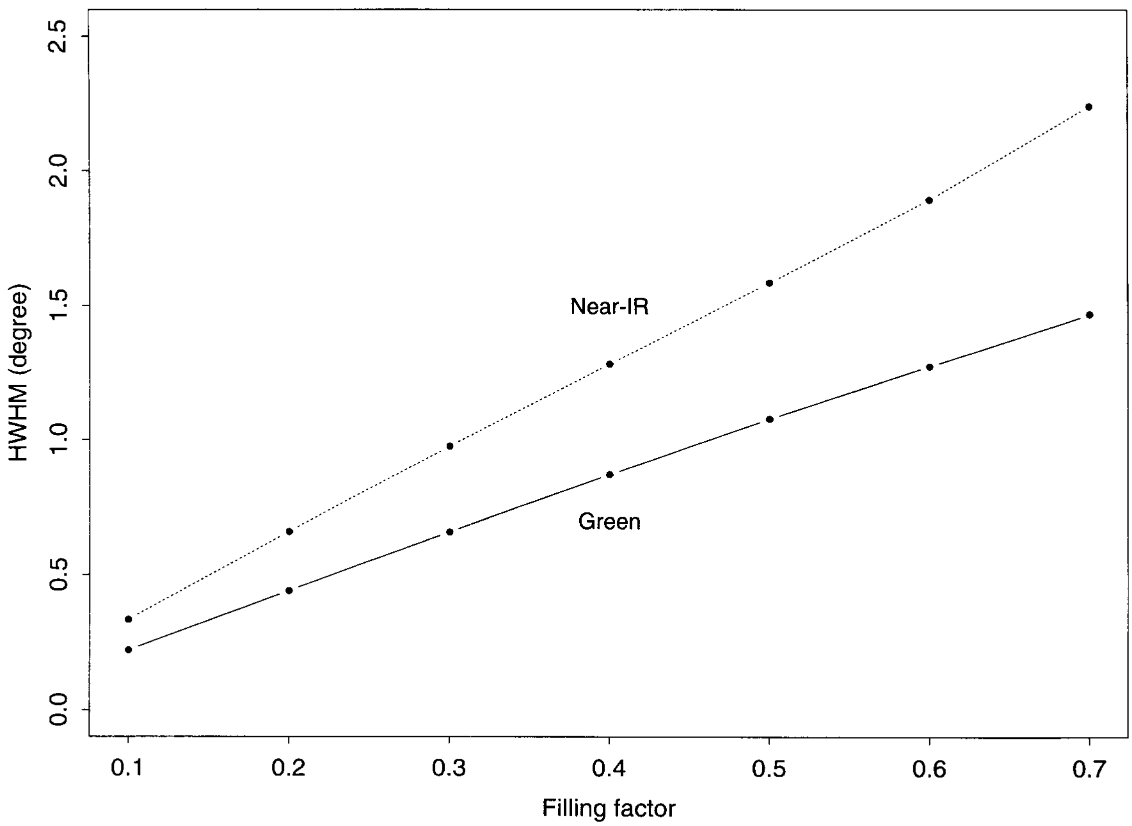

Figure 3. Angular width of the clay soil hot-spot with different filling factor values at green (0.533 μm, solid line) and near IR (0.817 μm, dotted line) wavelengths.

with controlled laboratory measurements (Wolf et al., 1988; van Albada et al., 1988). The theory is briefly summarized in the next section.

The angular width of the hot-spot peak depends on the ratio of the wavelength to the transport mean free path of photons in the medium. The half-width at half-maximum (HWHM) will be used to characterize the angular width of the coherent backscattering enhancement. The details of the computation taking into account the dense nature of the medium (Mishchenko, 1992b) are presented in the third section.

In the next two sections, the theoretical background for calculating both the magnitude and the angular width of the soil hot-spot effects is outlined. In the fourth section, the linkage with the Hapke empirical hot-spot function is discussed. Numerical experiments and data analyses are described in the fifth section. A brief discussion and conclusion are given in the final section.

CALCULATIONS OF THE HOT-SPOT MAGNITUDE

The original vector algorithm has been well described elsewhere (Mishchenko, 1992a). For ease of reference, the major formulas are summarized here.

Assume that the soil surface is illuminated by a parallel beam of light in the incident direction $\Omega_0(\theta_0, \varphi_0=0)$ and let $\mathbf{R}$ be the Stokes reflection matrix for exactly the backscattering direction $(\pi-\theta_0, \pi)$ and defined as

$$\cos\theta_0 \mathbf{R}\mathbf{I}^0=\pi\mathbf{I} \ ,$$

where $\mathbf{I}^0$ and $\mathbf{I}$ are the incident and reflected Stokes vectors, respectively. As discussed earlier, radiance in the backscattering direction is the sum of the single-scattering, incoherent multiple-scattering, and coherent components. Thus, the reflectance matrix can be written as

$$\mathbf{R}=\mathbf{R}^1+\mathbf{R}^m+\mathbf{R}^c \ .$$

It is very easy for us to calculate the single-scattering component $\mathbf{R}^1$:

$$\mathbf{R}^1=\frac{\omega\mathbf{P}(180°)}{8\cos\theta_0} \ ,$$

where ω is the single-scattering albedo and $\mathbf{P}(180°)$ is the single-scattering phase matrix of soil particles at the scattering angle 180°. For the incoherent multiple-scattering component $\mathbf{R}^m$, the conventional vector radiative transfer equation has to be solved. Different algorithms are available; the invariant imbedding algorithm (de Rooij, 1985; Mishchenko, 1990) is used in this study. No details are presented in this paper; the interested reader is referred to the original publications. After the calculation of $\mathbf{R}^1$ and $\mathbf{R}^m$, the coherent component can be calculated according to the following relation (Mishchenko, 1992a):

$$\mathbf{R}^c=\begin{bmatrix} R_{11}^c & R_{12}^m & 0 & 0 \\ R_{12}^m & R_{22}^c & 0 & 0 \\ 0 & 0 & R_{33}^c & R_{34}^m \\ 0 & 0 & -R_{34}^m & -R_{44}^c \end{bmatrix},$$

where

$$R_{11}^c=\frac{1}{2}(R_{11}^m+R_{22}^m-R_{33}^m+R_{44}^m),$$

$$R_{22}^c=\frac{1}{2}(R_{11}^m+R_{22}^m+R_{33}^m-R_{44}^m),$$

$$R_{33}^c=\frac{1}{2}(-R_{11}^m+R_{22}^m+R_{33}^m+R_{44}^m),$$

$$R_{44}^c=\frac{1}{2}(R_{11}^m-R_{22}^m+R_{33}^m+R_{44}^m),$$

and R_{ij}^m are the elements of the matrix $\mathbf{R}^m$. In this study, the enhancement factor ξ is considered only for unpolarized incident light with $\mathbf{I}^0=(1,0,0,0)^t$ where "t" stands for transpose. For more general definitions for the vector light, the reader is referred to the original paper (Mishchenko, 1992a). Similar to Eq. (1), the enhancement factor for the vector light can be defined as

$$\xi=\frac{R_{11}^1+R_{11}^m+R_{11}^c}{R_{11}^1+R_{11}^m}. \tag{3}$$

CALCULATION OF THE HOT-SPOT ANGULAR WIDTH

For a sparsely distributed medium with absorbing scatters, the half-width at half maximum (HWHM) of the soil hot-spot peak is defined as (Mishchenko, 1992b)

$$\mathrm{HWHM}=\frac{\varepsilon\lambda}{2\pi\lambda_{tr}}, \tag{4}$$

where

$$\lambda_{tr}^{-1}=NC_{ext}(1-\omega\langle\cos\theta\rangle),$$

ε is a constant close to 0.5 (Mishchenko and Dlugach, 1992b), and λ is the wavelength. In the preceding equation, N is the number of particles per unit volume, ω is the single scattering albedo, $\langle\cos\theta\rangle$ is the mean cosine of the scattering angle, and C_{ext} is the extinction cross section:

$$C_{ext}=C_{sca}+C_{abs},$$

where C_{sca} and C_{abs} are the scattering and absorbing cross sections, respectively. In this study, we modify the scattering cross section by considering the dense nature of the soil medium. The traditional definitions of C_{sca} and $C_{sca}\langle\cos\theta\rangle$ are (van de Hulst, 1981)

$$C_{sca}=\int_{4\pi} d\Omega\,\frac{dC_{sca}}{d\Omega},$$

$$C_{sca}\langle\cos\theta\rangle=\int_{4\pi} d\Omega\,\frac{dC_{sca}}{d\Omega}\cos\theta, \tag{5}$$

where $dC_{sca}/d\Omega$ is the differential scattering cross section and θ is the scattering angle. Notice that Eq. (4) is valid only for the normal incidence. For oblique incidence, HWHM increases as $1/\cos\theta_0$, where θ_0 is the incidence zenith angle (Gorodnichev et al., 1990).

Unlike aerosols in the atmosphere, particles in the soil medium are densely packed, and therefore spatial correlation among scattering particles should be taken into account. By introducing the structure factor $S(\theta)$, these two variables can be modified as follows:

$$C_{sca}=\int_{4\pi} d\Omega\,\frac{dC_{sca}}{d\Omega}S(\theta),$$

$$C_{sca}\langle\cos\theta\rangle=\int_{4\pi} d\Omega\,\frac{dC_{sca}}{d\Omega}\cos\theta S(\theta). \tag{6}$$

The structure factor has been widely used in the microwave remote sensing for dense-medium radiative transfer (Tsang et al., 1985; Kong, 1990). There are several different approaches for calculating the structure factor, $S(\theta)$; the Percus-Yevick approximation (Percus and Yevick, 1958) is used in this study:

$$S(\theta)=\frac{1}{[1-NC(p)]},$$

where

$$NC(p)=24f\left[\frac{(\alpha+\beta+\delta)}{u^2}\cos u-\frac{(\alpha+2\beta+4\delta)}{u^3}\sin u-\frac{2(\beta+6\delta)}{u^4}\cos u+\frac{2\beta}{u^4}+\frac{24\delta}{u^5}\sin u+\frac{24\delta}{u^6}(\cos u-1)\right],$$

$u=2pr_0$, r_0 is the average radius of the particles, and $p=[4\pi\sin(\theta/2)]/\lambda$. For the special case of $p=0$ (Mishchenko, 1992b),

$$NC(0)=24f(-\alpha/3-\beta/4-\delta/6),$$

where f is the filling factor:

$$f=\frac{4}{3}\pi Nr_0^3.$$

Other parameters are defined as:

$$\alpha=\frac{(1+2f)^2}{(1-f)^4}$$

$$\beta=-6f\frac{(1+f/2)^2}{(1-f)^4}$$

$$\delta=\alpha f/2$$

CALCULATION OF SOIL OPTICAL PROPERTIES

To calculate the hot-spot magnitude and angular width, we need to know the single-scattering albedo, scattering matrix, and differential-scattering cross section of the soil medium. The soil particle distribution can be repre-

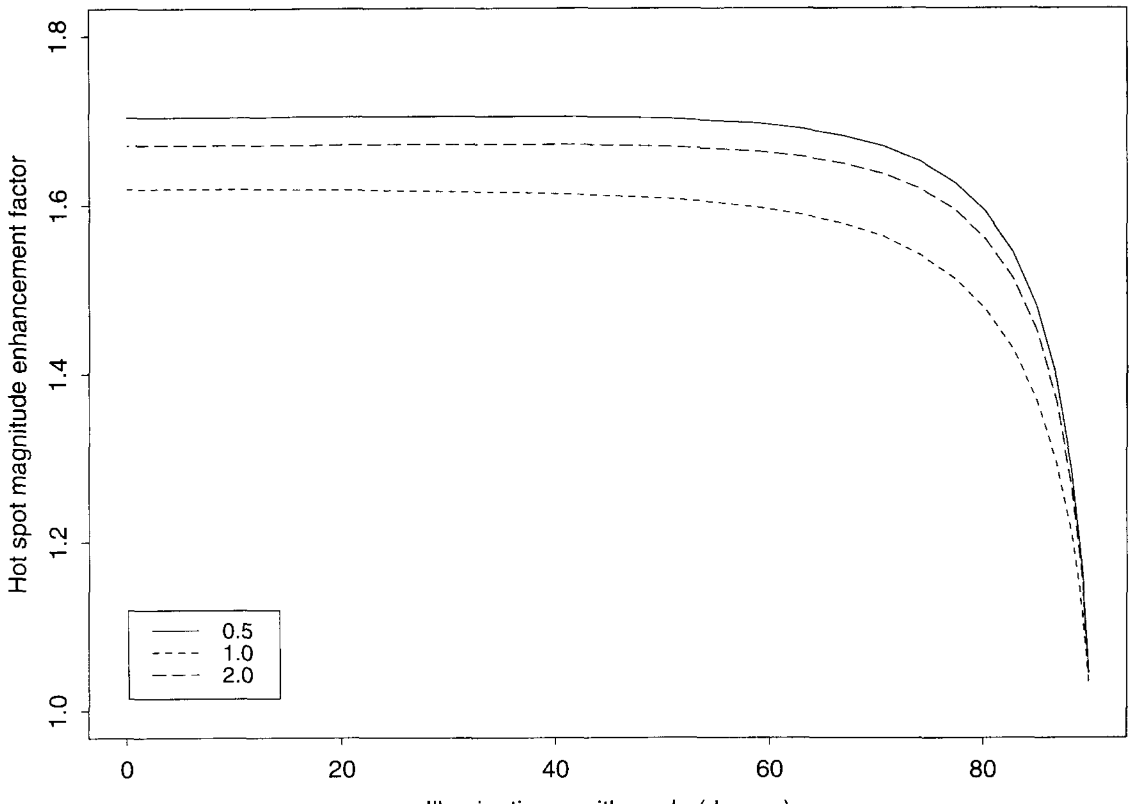

a

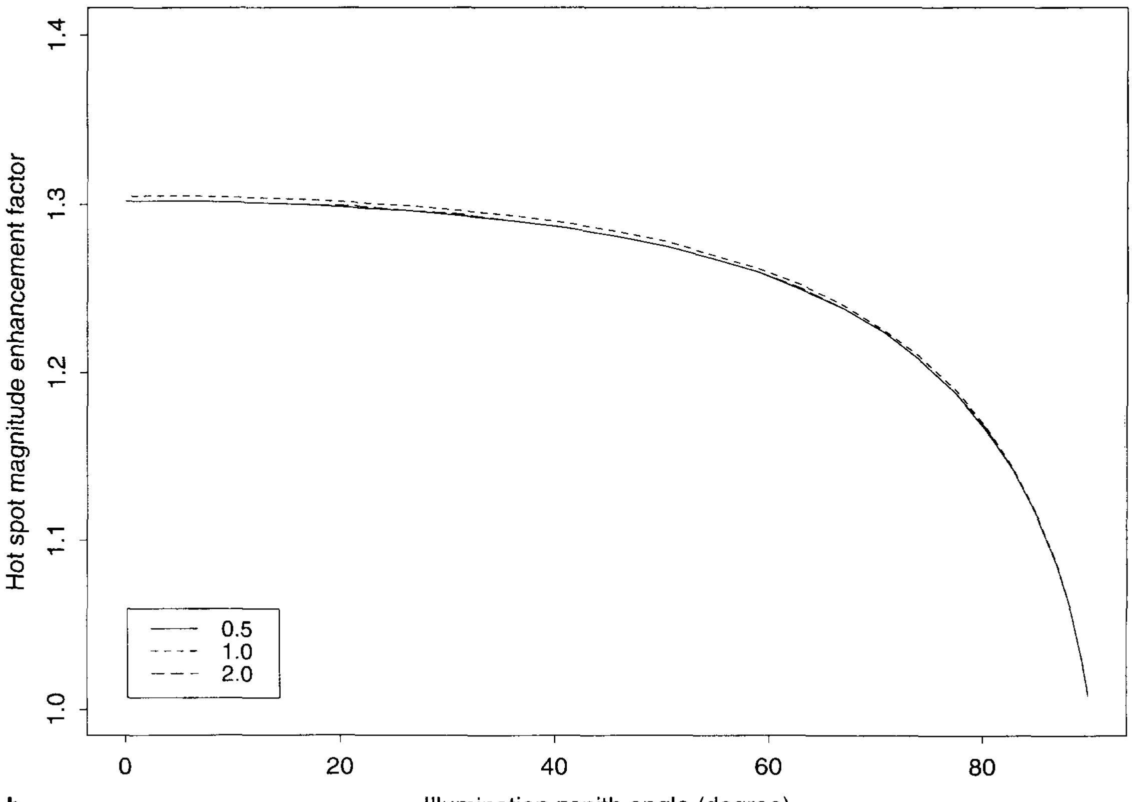

b

Figure 4. Effects of soil particle shapes on the enhancement factor of the hot-spot effect; (a) coarse clay, (b) fine clay. Soil particle shapes are assumed to be ellipsoidal with different shape ratios.

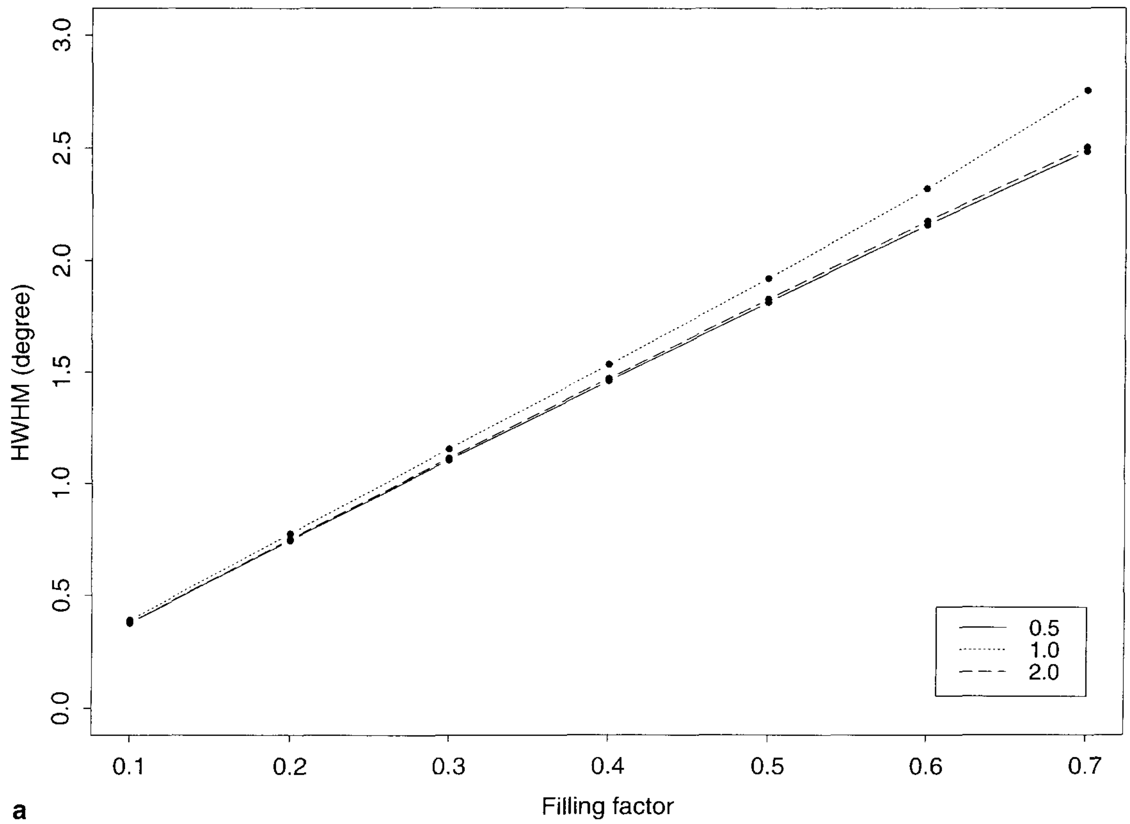

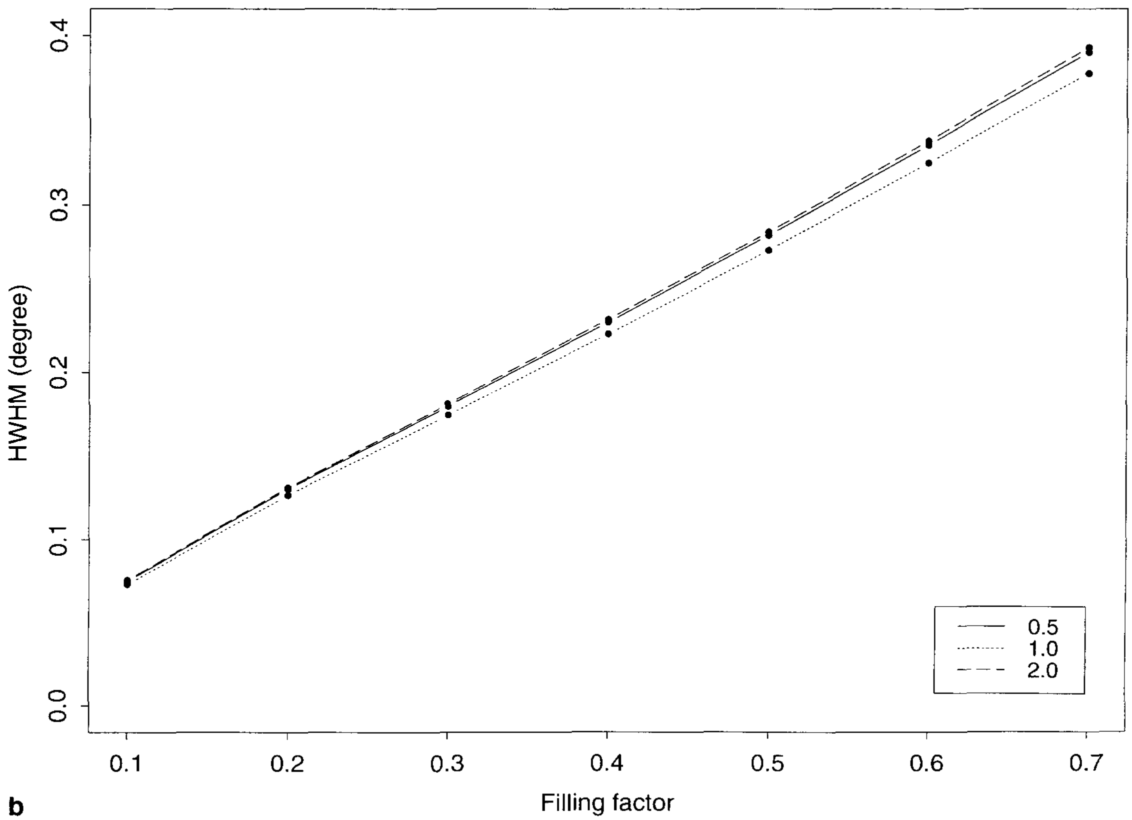

Figure 5. Effects of soil particle shapes on the angular width of the hot-spot effect: (a) coarse clay; and (b) fine clay.

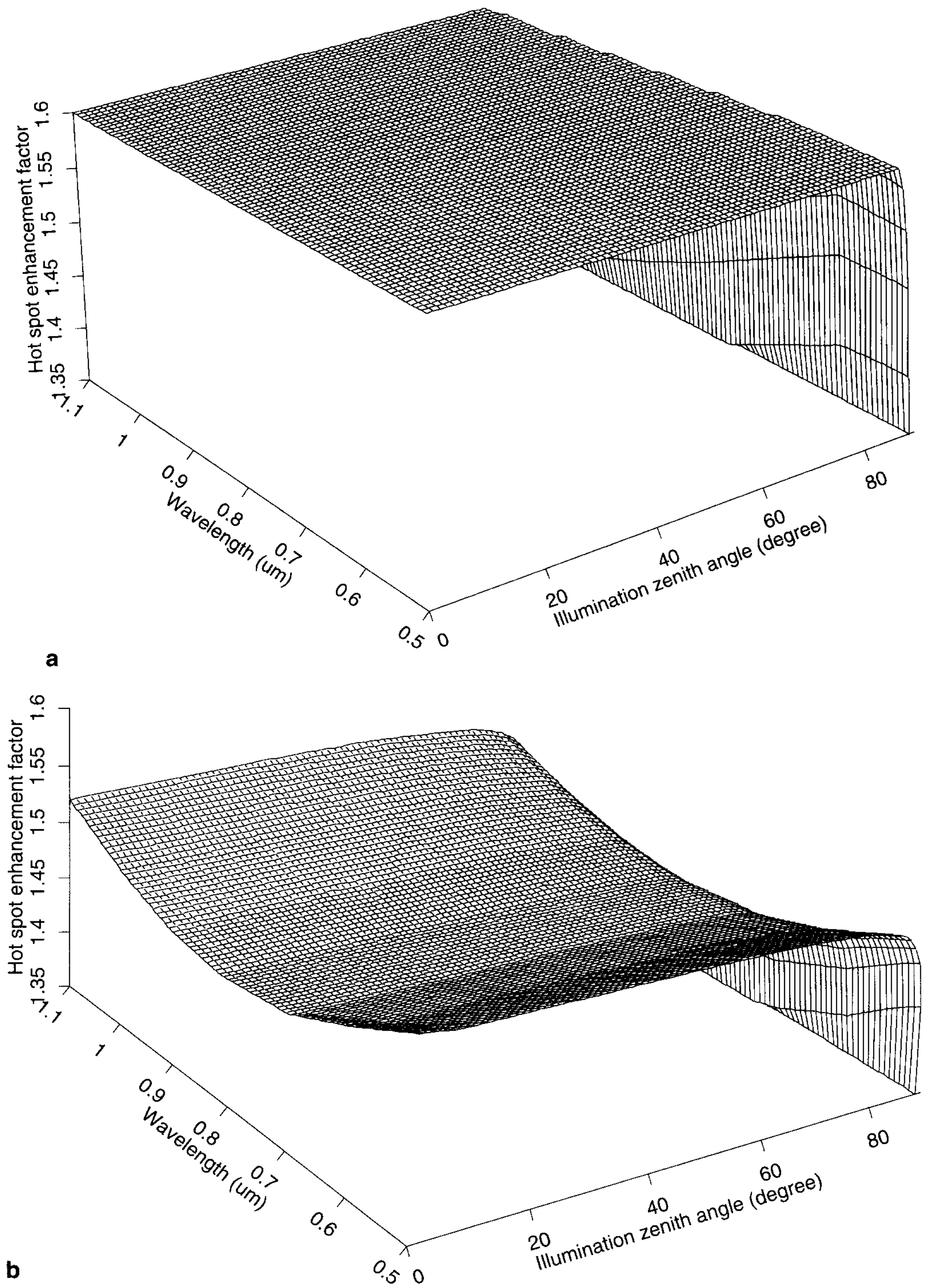

Figure 6. Wavelength dependence of the hot spot enhancement factor for (a) clay and (b) fine silt soils.

sented by different functions, such as lognormal (Buchan, 1989) and Rosin (Dapples, 1975) distributions. For simplicity, the soil particle size distribution in this study is assumed to follow the power law (Hansen and Travis, 1974):

$$n(r)=\frac{2r_{\min}^2\, r_{\max}^2}{r_{\max}^2-r_{\min}^2}r^{-3} \ ,$$

where the particle radius lies in the range $(r_{\min}, r_{\max})$. This distribution is often characterized by the effective equal-volume-sphere radius r_{eff} and the effective variance v_{eff}:

$$r_{\text{eff}}=\frac{r_{\max}-r_{\min}}{\ln(r_{\max}/r_{\min})}$$

$$v_{\text{eff}}=\frac{r_{\max}+r_{\min}}{2(r_{\max}-r_{\min})}\ln\,(r_{\max}/r_{\min})-1 \ .$$

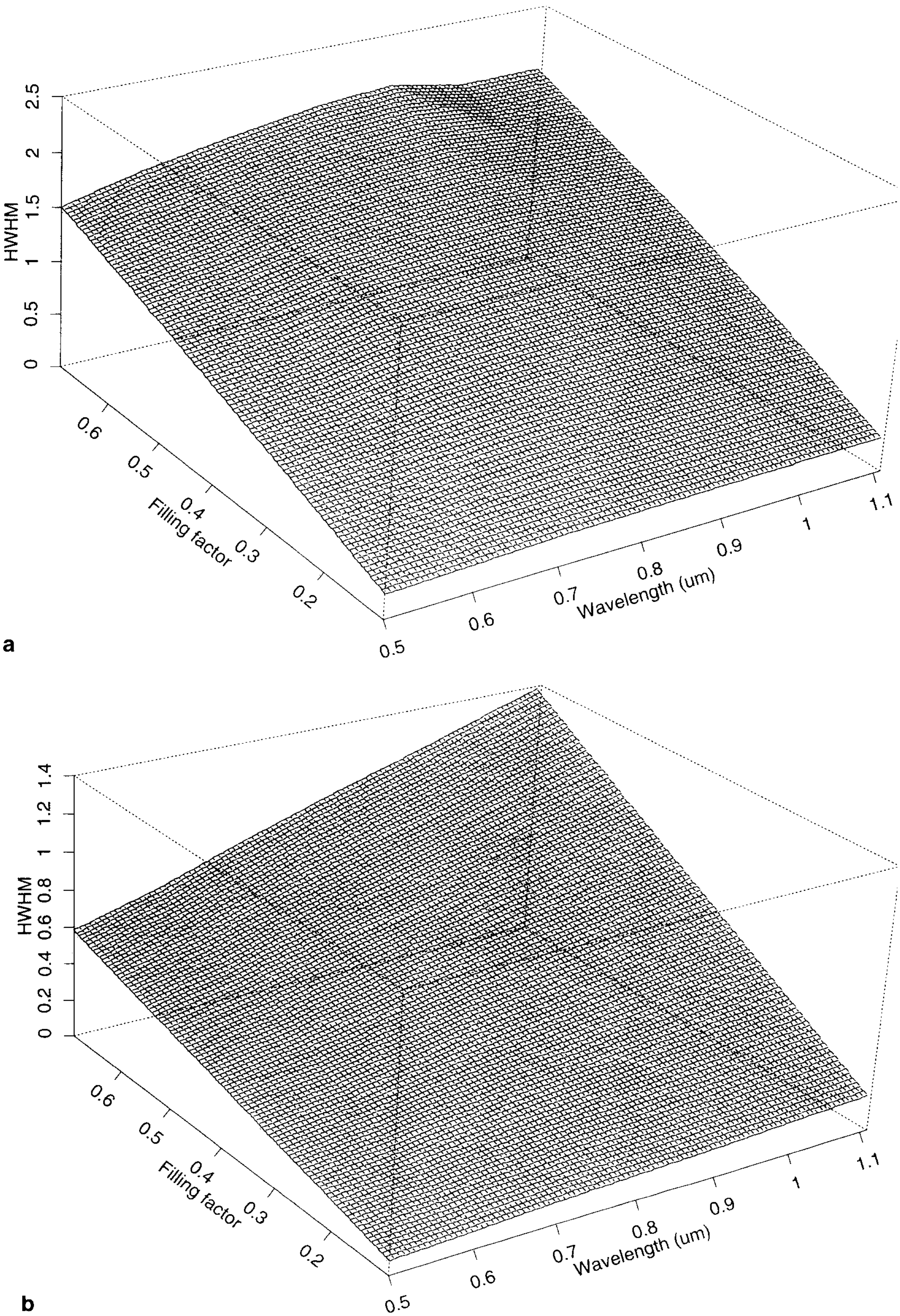

Figure 7. Wavelength dependence of the hot-spot angular width for (a) clay and (b) fine silt soils.

Individual soil particles are assumed to be randomly oriented ellipsoids. The equation of an ellipsoidal surface can be expressed in the spherical coordinate system as

$$r(\theta,\varphi)=a(\sin^2\theta+d^2\cos^2\theta)^{-1/2} \ ,$$

where $d=b/a$ the ratio of the semiaxes of the ellipsoid. We can describe the particle shapes ranging from needles ($d<<1$) to disks ($d>>1$) by varying the shape parameter, d. If $d=1$, the particle is spherical, and thus Mie theory can be used for calculating those optical properties. For ellipsoidal particles, the T-matrix approach (Mishchenko, 1991, 1993, Mishchenko et al., 1996) is used in this study. No details are given in this paper; interested readers are referred to the original articles.

The gamma size distribution for soil particles also is used in this study:

$$n(r)=C\ r^{(1-3v_{eff})/v_{eff}} \exp[-r/(r_{eff}v_{eff})] \ ,$$

where C is a normalization constant.

LINKAGE WITH THE HAPKE EMPIRICAL FORMULA

Hapke (1986) derived a rigorous equation based on the shadowing theory and then gave a semiempirical function as an approximation for describing the hot spot, which is quite popular in the environmental remote-sensing community:

$$B(a)=\frac{B_0}{1+\tan(a/2)/h} \ ,$$

where a is the phase angle between the illumination direction Ω_0 and the viewing direction Ω, and B_0 and h are two parameters for the height and the angular width of the hot-spot peak. Although it was derived from the shadowing theory, its final form essentially is a statistical formula. A straightforward linkage between this formula and the hot-spot magnitude and angular width discussed in the preceding sections can be given:

$$\begin{aligned} B_0&=\xi \ , \\ h&=\tan(\mathrm{HWHM}/2) \ . \end{aligned} \qquad (7)$$

Similar efforts have been independently reported (Helfenstein et al., 1996). Caution has to be taken when calculating the real reflectance in the hot-spot region. The reflectance in the backscattering direction is equal to $[1+B(\theta)]R^1$ according to the shadowing theory, whereas it should be $[1+B(\theta)]R$ according to coherent backscattering theory, where R^1 and R are the single-scattering reflectance and the total incoherent reflectance (single plus incoherent multiple scattering). This emphasizes one of the major differences between the shadowing theory and the coherent backscattering theory in that the former depends mainly on single scattering, whereas the latter is based on multiple scattering.

NUMERICAL EXPERIMENTS AND DATA ANALYSIS

Coherent backscattering is a universal interference phenomenon and occurs for particles of any size (Barabanenkov et al., 1991). However, in some cases, the hot-spot peak can have a very small amplitude or angular width, which can make it unobservable (Mishchenko, 1992b; Hapke and Blewett, 1991). Therefore, various questions remain when it is applied to soils regarding its validity range, wavelength dependence, soil particle shape effect, and so on. To answer these questions, a series of numerical experiments have been designed and carried out with the use of the measured refractive indices of the particles. The calculated results and evaluations are as follows.

The first case is designed to examine how the hot-spot parameters of a clay soil vary at different solar illumination angles and different filling factor values at two wavelengths (green, 0.553 μm, and near infrared (IR), 0.817 μm). The soil refractive indices are $1.524+i0.01265$ for the green and $1.527+i0.02044$ for the near IR, which were measured for montmorillonite particles at Clay Spur, Wyoming (Egan and Hilgeman, 1979). Particles are assumed to be spherical with the size distribution of the gamma law. Let $r_{\mathrm{eff}}=0.5$ μm and $v_{\mathrm{eff}}=0.2$; the program samples particles with diameters ranging from 0.4 μm to 2 μm. Figure 2 illustrates the hot-spot magnitude enhancement factor, ξ, calculated from formula (3). Although the enhancement factors at different wavelengths have different magnitudes, both are insensitive to the solar zenith angle up to 70°. When the solar zenith angle is larger than 70°, the enhancement factor decreases dramatically because the multiply scattered component decreases for large incident angles. Figure 3 presents the HWHM for the same type of soils at different filling factor values. The angular width of the hot-spot peak becomes larger when the soil medium becomes denser. HWHM at the near-IR wavelength is obviously much larger than that at the green wavelength. This observation is somewhat different from the shadowing theory prediction that the angular width of the hot-spot peak is very insensitive to the wavelength. It also is independent of the illumination angle.

The second case is designed to evaluate the effect of the soil particle shapes. In accord with the European soil classification system, the clay is further divided into coarse clay (diameters ranging from 0.0006 to 0.002 mm), medium clay (diameters ranging from 0.0002 to 0.0006 mm), and fine clay (diameters<0.0002 mm). Particle sizes are assumed to follow the power law. Figure 4 presents the calculated enhancement factor for both the coarse clay ($r_{\mathrm{eff}}=0.65$ μm and $v_{\mathrm{eff}}=0.1$) and the fine clay ($r_{\mathrm{eff}}=0.05$ μm and $v_{\mathrm{eff}}=0.2$) at three shape ratios of b/a, where a is the length of the semiaxis of rotational symmetry for the ellipsoids and b is the length of the

Table 1. Soil Refractive Indices ($n_r+i\ n_i$)

Wavelength (μm)	n_r	n_i
0.500	1.415	0.05029
0.600	1.411	0.04289
0.700	1.399	0.05393
0.817	1.395	0.05448
0.907	1.391	0.05393
1.000	1.387	0.05448
1.105	1.387	0.05340

other semiaxis. Figure 4a shows that the enhancement factor of the coarse clay is sensitive to the particle shape, and nonspherical particles have a larger enhancement factor. The difference is as large as 6%. However, the fine clay soils with different shapes do not produce any significant differences (Fig. 4b). Figure 5 reveals a very interesting result: nonspherical particles of the coarse clay generate smaller angular widths than do spherical particles, but nonspherical particles of the fine clay produce larger angular widths.

The third case is designed to examine the wavelength dependence. The refractive indices are listed in Table 1. They were measured for illite particles from Fithian, Illinois (Egan and Hilgeman, 1979). The parameters of the gamma distribution are $r_{\text{eff}}=0.5\ \mu m$ and $v_{\text{eff}}=0.2$ for clay soils and $r_{\text{eff}}=0.75\ \mu m$ and $v_{\text{eff}}=0.1$ for fine silt soils. The calculated enhancement factor is displayed in Figure 6. The enhancement factor remains almost constant in the visible and near-IR spectrum. The wavelength dependence of the angular width for the clay soils (Fig. 7), however, is stronger than that of the enhancement factor. The effect of the refractive index is evident when the filling factor is large. For fine silt soils, the wavelength dependence of both angular width and magnitude is much stronger than for the clay soils. We have actually demonstrated the very important fact that the angular width is very sensitive to the ratio of the particle radius to the wavelength (Mishchenko, 1992b). If the ratio is too small or too large, the angular width of the hot spot is not significant.

DISCUSSION AND CONCLUSIONS

The coherent backscattering theory is used to calculate the magnitude and angular width of the soil hot-spot effect. The soil particle size is assumed to follow the power law and gamma distributions, and individual particles are assumed to be spheres and ellipsoids. The T-matrix approach is used to calculate the optical properties (i.e., single-scattering albedo, scattering matrix, differential scattering cross section, etc.) of the nonspherical particles. The soil structure is characterized by the filling factor (i.e., the percentage of the particle occupancy). The vector radiative transfer equation is solved by the fast invariant imbedding method. The variables are also linked to the coefficients of the Hapke hot-spot semiempirical function simplified from the derivation based on the shadowing theory.

Because the optical mechanisms of the coherent backscattering theory and the shadowing theory are completely different, the calculated results reveal several important differences. First, the predicted soil hot-spot effect based on the coherent backscattering theory primarily depends on multiple scattering; therefore the magnitude of the soil hot-spot peak increases as the reflectance increases, which is a strong function of the wavelength. Conversely, the predicted magnitude of the soil hot-spot peak based on the shadowing theory decreases as the reflectance increases because shadow hiding is important only for singly scattered light. Second, the angular width of the coherent backscattering peak is a function of the wavelength (more specifically, the ratio of the particle radius to the wavelength), whereas the shadow hiding peak is independent of the wavelength, provided that the wavelength is much smaller than the particle size.

The numerical calculations in this study show that the magnitude of the soil hot-spot effect is insensitive to the solar zenith angle, θ_0, up to $\theta_0\approx70°$. It is demonstrated that the soil hot spot is sensitive to the particle shape and the filling factor. Theoretically, those important soil properties may be retrieved from hot-spot observations. Practically, the current radiometers used for environmental remote sensing have much larger fields of view, which may largely change the observed angular shape and magnitude of the soil hot spot. The soil refractive index is another parameter controlling the hot-spot shape. The shape is much more sensitive to the imaginary part. More investigations on this subject are needed. Another problem is that the hot spot may be caused by other factors—for example, the surface roughness. Therefore, further theoretical and experimental studies are highly required to understand similarities and differences in the hot-spot phenomena produced by different optical mechanisms.

The authors are grateful to Drs. Bruce Hapke and Andres Kuusk for reviewing a preliminary version of the manuscript.

REFERENCES

Barabanenkov, Y. N., Kravtsov, Y. A., Ozrin, V. D., and Saichev, A. I. (1991), Enhanced backscattering in optics. In *Progress in Optics*, Vol. 29 (E. Wolf, Ed.), Elsevier, New York, pp. 65–197.

Breon, F. M., Vanderbilt, V., Leroy, M., Bicheron, P., Walthall, C. L., and Kalshovens, J. E. (1996). Evidence of hot spot directional signature from airborne POLDER measurements. Submitted to *IEEE Trans. Geosci. Remote Sens.*

Buchan, G. D. (1989), Applicability of the simple lognormal model to particle-size distribution in soils. *Soil Sci.* 147: 155–161.

Dapples, E. C. (1975), Laws of distribution applied to sand sizes. *Geol. Soc. Am. Mem.* 142:37–61.

Deering, D. W., Middleton, E. M., and Eck, T. F. (1994), Reflectance anisotropy for a Spruce-Hemlock forest canopy. *Remote Sens. Environ.* 47:242–260.

de Rooij, W. A. (1985), *Reflectance and transmission of polarized light by planetary atmospheres.* Ph.D. Thesis, Free University, Amsterdam.

Egan, W. G., and Hilgeman, T. W. (1979), *Optical Properties of Inhomogeneous Materials: Applications to Geology, Astronomy, Chemistry, and Engineering.* Academic Press, New York.

Gerstl, S. A. W., Simmer, C., and Powers, B. J. (1986), The canopy hot spot as a crop identifier. *Proceedings of the Symposium on Remote Sensing for Resources Development and Environmental Management*, 261–263, 1986, Enschede.

Gorodnichev, E. E., Dudarev, S. L., and Rogozkin, D. B. (1990), Coherent wave backscattering by random medium: exact solution of the albedo problem. *Phys. Lett.* 144:48–54.

Hansen, J. E., and Travis, L. D. (1974), Light scattering in planetary atmospheres. *Space Sci. Rev.* 16:527–610.

Hapke, B. W. (1981), Bidirectional reflectance spectroscopy, 1: theory. *J. Geophys. Res.* 86:3039–3054.

Hapke, B. (1986), Bidirectional reflectance spectroscopy, 4: the extinction coefficient and the opposition effect. *Icarus* 67:264–280.

Hapke, B., and Blewett, D. (1991), Coherent backscatter model for the unusual radar reflectivity of icy satellites. *Nature* 352:46–47.

Hapke, B., Dominick, D., Nelson, R., and Smythe, W. (1996), The cause of the hot spot in vegetation canopies and soils: shadow-hiding versus coherent backscattering. *Remote Sens. Environ.* 58:63–68.

Helfentstein, P., Veverka, J., and Hillier, J. (1996), Monochromatic photometry of the moon and the lunar opposition effect. Submitted to *Icarus*.

Irons, J. R., Ranson, K. J., Williams, D. L., Irish, R. R., and Huegel, F. G. (1991), An off-nadir pointing imaging spectroradiometer for terrestrial ecosystem studies. *IEEE Trans. Geosci. Remote Sens.* 29:66–74.

Jacquemoud, S., Baret, F., and Hanocq, J. F. (1992), Modeling spectral and bidirectional soil reflectance. *Remote Sens. Environ.* 41:123–132.

Jupp, D. L. B., and Strahler, A. H. (1991), A hot spot model for leaf canopies. *Remote Sens. Environ.* 38:193–210.

Jupp, D. L. B., Walker, J., and Penridge, L. K. (1986), Interpretation of vegetation structure in Landsat MSS imagery: a case study in disturbed semi-arid euclypt woodlands, 2: model-based analysis. *J. Environ. Manage.* 23:35–57.

Kong, J. A. (1990), *Electromagnetic Wave Theory.* Wiley, New York.

Kuusk, A. (1985), The hot spot effect of a uniform vegetation cover. *Sov. J. Remote Sens.* 3:645–658.

Liang, S., and Townshend, J. R. G. (1996a), A parametric soil BRDF model: a four-stream approximation. *Int. J. Remote Sens.* 17:1303–1315.

Liang, S., and Townshend, J. R. G. (1996b), A modified Hapke model for soil bidirectional reflectance. *Remote Sens. Environ.* 55:1–10.

Lumme, K., Peltoniemi, J., and Irvine, W. M. (1990), Some photometric techniques for atmosphereless solar system bodies. *Adv. Space Res.* 10:187–193.

Mishchenko, M. I. (1990), The fast invariant imbedding method for polarized light: computational aspects and numerical results for Rayleigh scattering. *J. Quant. Spectrosc. Radiat. Transfer* 43:163–171.

Mishchenko, M. I. (1991), Light scattering by randomly oriented axially symmetric particles. *J. Opt. Soc. Am.* A8: 871–882.

Mishchenko, M. I. (1992a), Enhanced backscattering of polarized light from discrete random media: calculations in exactly the backscattering direction. *J. Opt. Soc. Am.* A9: 978–982.

Mishchenko, M. I. (1992b), The angular width of the coherent backscattering opposition effect: an application to icy outer planet satellites. *Astrophys. Space Sci.* 194:327–333.

Mishchenko, M. I. (1993), Light scattering by size-shape distributions of randomly oriented axially symmetric particles of a size comparable to a wavelength. *Appl. Opt.* 32:4652–4666.

Mishchenko, M. I., and Dlugach, J. M. (1992a), The amplitude of the opposition effect due to weak localization of photons in discrete random media. *Astrophys. Space Sci.* 189: 151–154.

Mishchenko, M. I., and Dlugach, J. M. (1992b), Can weak localization of photons explain the opposition effect of Saturn's rings? *Mon. Not. R. Astr. Sco.* 254:15p–18p.

Mishchenko, M. I., and Dlugach, J. M. (1993), Coherent backscatter and the opposition effect for E-type asteroids. *Planet. Space Sci.* 41:173–181.

Mishchenko, M. I., Travis, L. D., and Mackowski, A. W. (1996), T-Matrix computations of light scattering by nonspherical particles: a review. *J. Quant. Spectrosc. Radiat. Transfer* 55:535–575.

Qin, W., and Xiang, Y. (1994), On the hotspot effect of leaf canopies: modeling study and influence of leaf shape. *Remote Sens. Environ.* 50:95–106.

Percus, J., and Yevick, G. (1958), Analysis of classical statistical mechanics by means of collective coordinates. *Phys. Rev.* 110:1–13.

Peters, K. J. (1992), Coherent-backscatter effect: a vector formulation accounting for polarization and absorption effects and small or large scatters. *Phys. Rev.* B46:801–812.

Ranson, K. J., Irons, J. R., and Williams, D. L. (1994), Multispectral bidirectional reflectance of northern forest canopies with the advanced solid state array spectroradiometer (ASAS). *Remote Sens. Environ.* 47:276–289.

Tsang, L., Kong, J. A., and Shin, R. T. (1985), *Theory of Microwave Remote Sensing.* Wiley-Interscience, New York.

van Albada, M. P., van de Mark, M. B., and Lagendijk, A. (1988), Polarization effects in weak localization of light. *J. Phys.* D21:S28–S31.

van de Hulst, H. C. (1981), *Light Scattering by Small Particles.* Dover, New York.

Verstraete, M. M., Pinty, B., and Dickinson, R. E. (1990), A physical model of the bidirectional reflectance of vegetation canopies, 1: theory. *J. Geophys. Res.* 95:11,755–11,765.

Wolf, P. E., Maret, G., Akkermans, E., and Maynard, R. (1988), Optical coherent backscattering by random media: an experimental study. *J. Phys. France* 49:63–75.